Influence of polydispersity on dynamic light scattering measurements on concentrated suspensions

A. van Veluwen, H. N. W. Lekkerkerker, C. G. de Kruif, and A. Vrij
Van't Hoff Laboratory, University of Utrecht, Padualaan 8, 3584 CH Utrecht, The Netherlands

(Received 29 December 1987; accepted 31 May 1988)

The dynamic structure factor for concentrated dispersions of small polydisperse hard spherical particles has been measured and compared with theoretical predictions. Experimental evidence for the occurrence of a slowly decaying mode has been found. The dynamic structure factor is analyzed in terms of two independent modes, associated with collective diffusion and exchange diffusion. Calculations of the mode amplitudes are extended to the case of combined optical and size polydispersity. The correspondence between measurements and theory is quite satisfactory.

I. INTRODUCTION

In recent years there has been a large increase of activity in the study of concentrated colloidal dispersions by dynamic light scattering.[1,2] A large part of these activities has been focused on monodisperse colloidal particles, where detailed data interpretation is frequently possible. For these systems much theoretical and experimental progress has indeed been made. While these monodisperse systems are interesting in their own right, they do not occur as widely as concentrated suspensions of polydisperse particles. It has been pointed out[3,4] that even a small degree of polydispersity can have profound effects on the dynamic light scattering (DLS) of concentrated suspensions.

The analysis of DLS experiments on systems of concentrated polydisperse particles, however, is not as firmly established as it is for systems of monodisperse particles, and frequently approximate approaches have to be employed. In 1982 Pusey, Fijnaut, and Vrij[4] argued that the light scattering intensity autocorrelation function consists of two independent modes with well-separated decay times. The faster decaying mode was identified with collective stochastic compression–dilation motions, or collective diffusion, and is present even for a monodisperse system; the slower decaying mode describes the exchange of particles of different types, closely related to long-time self-diffusion. An important quantitative result of their work was the calculation of the relative mode amplitudes. Although convincing, their theory is intuitive rather than rigorous and it still needs experimental verification.

The aim of this paper is twofold. First, we extend the calculations of Pusey *et al.*[4] concerning the mode amplitudes to the case of combined optical and size polydispersity. Second, we present DLS measurements on two systems of small polydisperse particles (average radii 10 and 22 nm, respectively) that we analyzed in terms of the expected mode separation. We found that with increasing concentration the electric field autocorrelation function is indeed composed of two modes with well separated decay times. These decay times satisfy the expected concentration-dependent behavior of the collective and exchange diffusion. Particularly, the exchange diffusion was found to be a very sensitive function of concentration.

After a preliminary introduction on DLS in Sec. II A, we review in Secs. II B and II C the existing theory for the cases of pure optical and pure size polydispersity, respectively. In Sec. II D we describe the calculation of the mode amplitudes in the case of combined optical and size polydispersity. In Sec. III we describe the two systems used in the experiments, followed by a discussion of the light scattering method. The results of the experiments are discussed in Sec. IV.

II. THEORY

A. Preliminaries

We consider scattering from a volume V containing N small spherical particles. For large N, dynamic light scattering provides an experimental estimate of $g^{(1)}(\tau)$, the normalized time correlation function of the electric field amplitude E:

$$g^{(1)}(q,\tau)=\frac{\langle E(q,0)E^*(q,\tau)\rangle}{\langle|E(q,0)|^2\rangle}=\frac{F^M(q,\tau)}{S^M(q)}. \tag{1}$$

Here τ is the correlation delay time and $F^M(q,\tau)$ is the measured dynamic structure factor at scattering vector $q=(4\pi n/\lambda_0)\sin(\theta/2)$, where λ_0 is the wavelength of the light *in vacuo*, n is the refractive index of the suspension, and θ is the scattering angle. The measured static structure factor is $S^M(q)=F^M(q,0)$. For rigid spherical particles the measured dynamic structure factor is given by[1]

$$F^M(q,\tau)=[N\bar{f}^2]^{-1}\sum_i\sum_j f_i f_j\langle\exp\{i\mathbf{q}\cdot[\mathbf{r}_i(0)-\mathbf{r}_j(\tau)]\}\rangle, \tag{2}$$

where f_j is the scattering amplitude of particle j and $\mathbf{r}_j(\tau)$ is its position at time τ.

In the following, angular brackets indicate an ensemble average over all possible particle positions, whereas a bar indicates a number averaged quantity. Accordingly, the average scattering amplitude is given by

$$\bar{f}\equiv N^{-1}\sum_{i=1}^{N} f_i \tag{3}$$

and the mean-square scattering amplitude is

 0021-9606/88/172810-06$02.10

$$\overline{f^2} \equiv N^{-1} \sum_{i=1}^{N} f_i^2 . \tag{4}$$

B. Optical polydispersity

If the particles are identical in terms of size and interactions, but differ in scattering power, then the expression for F^M can be separated into ensemble averages and number averages.[1,4] This yields

$$F^M(q,\tau) = (1-x)F(q,\tau) + xF_s(q,\tau) , \tag{5}$$

where

$$F(q,\tau) = N^{-1} \sum_{i,j=1}^{N} \langle \exp\{i\mathbf{q}\cdot[\mathbf{r}_i(0) - \mathbf{r}_j(\tau)]\}\rangle \tag{6}$$

is the full dynamic structure factor and

$$F_s(q,\tau) = \langle \exp\{i\mathbf{q}\cdot[\mathbf{r}(0) - \mathbf{r}(\tau)]\}\rangle \tag{7}$$

is the self-dynamic structure factor. The quantity x is a measure of the optical polydispersity

$$x = 1 - \bar{f}^2/\overline{f^2} = \sigma_f^2/(1+\sigma_f^2) , \tag{8}$$

where σ_f is the relative standard deviation in scattering amplitude

$$\sigma_f^2 = (\overline{f^2} - \bar{f}^2)/\bar{f}^2 .$$

In the limit $qa \to 0$, where a is the particle radius, the full-dynamic structure factor describes collective diffusion, driven by osmotic pressure gradients, whereas the self-dynamic structure factor describes long-time self-diffusion. In this limit the measured dynamic structure factor becomes

$$\lim_{qa\to 0} F^M(q,\tau) = (1-x)S^I(0)\exp(-D_c q^2 \tau) + x\exp(-D_s q^2 \tau) , \tag{9}$$

where D_c is the collective diffusion coefficient, D_s is the long-time self-diffusion coefficient, and $S^I(q)$ is the static structure factor of the "ideal" monodisperse system.

For $\tau = 0$, Eq. (9) reduces to

$$S^M(0) = (1-x)S^I(0) + x = A_+ + A_- . \tag{10}$$

The amplitude of the "self-mode" is $A_- = x$ and the amplitude of the "collective mode" is

$$A_+ = (1-x)S^I(0) = \frac{\bar{f}^2}{\overline{f^2}} kT \left(\frac{\partial \rho}{\partial \Pi}\right)_{T,\mu_0} , \tag{11}$$

where Π is the osmotic pressure, T is the absolute temperature and μ_0 is the chemical potential of the solvent. In Fig. 1(a) we plot the relative amplitude $A_-/(A_- + A_+) = x/[x + (1-x)S^I(0)]$ as a function of volume fraction ϕ for various values of the standard deviation σ_f. For $S^I(0)$ we take

$$S^I(0) = (1-\phi)^4/(1+2\phi)^2 , \tag{12}$$

the result of the Percus–Yevick approximation for monodisperse hard spheres at volume fraction ϕ.

The theory for pure optical polydispersity applies to particles which differ in refractive index only. So

$$(\overline{f^2} - \bar{f}^2) \propto (\overline{n^2} - \bar{n}^2) \quad \text{and} \quad \bar{f} \propto (\bar{n} - n_0) ,$$

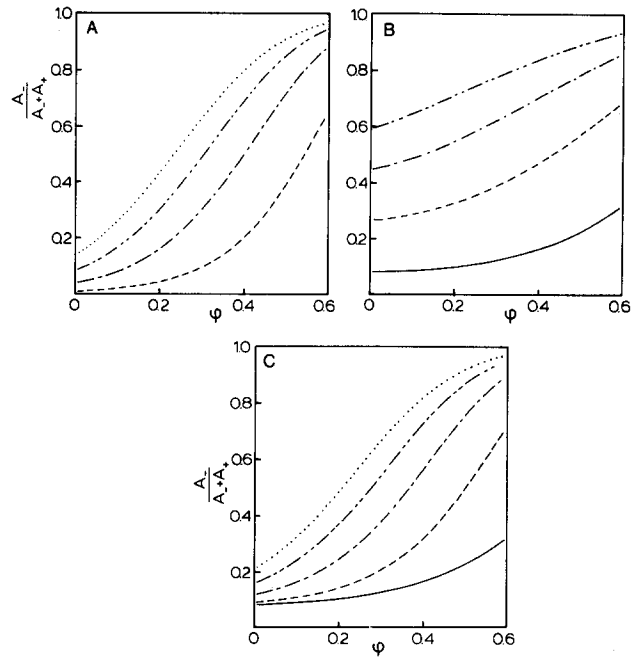

FIG. 1. Comparison of theoretical predictions for the relative amplitude of the slow mode as a function of the volume fraction of the hard spheres for various values of the standard deviations in the cases of: (a) pure scattering power (= optical) polydispersity for $\sigma_f(=\sigma_b) = 0.10$ (- - -), $\sigma_f = 0.20$ (- - -), $\sigma_f = 0.30$ (- - - -), and $\sigma_f = 0.40$ (···); (b) pure size polydispersity for $\sigma_a = 0.10$ (—), $\sigma_a = 0.20$ (- - -), $\sigma_a = 0.30$ (- - -), and $\sigma_a = 0.40$ (- - - -); (c) combined size and optical polydispersity for $\sigma_a = 0.10$ combined with $\sigma_b = 0$ (—), $\sigma_b = 0.10$ (- - -), $\sigma_b = 0.20$ (- - -), $\sigma_b = 0.30$ (- - - -), and $\sigma_b = 0.40$ (···).

where n and n_0 refer to the refractive indices of the particles and the solvent, respectively. The scattered intensity is minimal under a refractive index matching condition, i.e., when

$$n_0 = \bar{n} ,$$

in which case $x = 1$. More generally, it can be shown that x equals the ratio of the scattered intensity in the matchpoint to the measured scattered intensity, provided these measurements were taken with the same dilute sample. This can be used as a rule of thumb to estimate the influence of optical polydispersity.

C. Size polydispersity

A system of particles polydisperse in size but with the same refractive index, can be characterized by a standard deviation in size σ_a given by

$$\sigma_a^2 = (\overline{a^2} - \bar{a}^2)/\bar{a}^2 .$$

The scattering amplitudes $f_i \propto a_i^3$ and so

$$F^M(q,\tau) = [N\,\overline{a^6}]^{-1} \left\langle \sum_i \sum_j a_i^3 a_j^3 \exp\{i\mathbf{q}\cdot[\mathbf{r}_i(0) - \mathbf{r}_j(\tau)]\}\right\rangle . \tag{13}$$

Unlike the case of pure optical polydispersity, this expression cannot be further separated into ensemble averages over particle positions and number averages over the scattering amplitudes, because generally there exists a strong correlation between the particle radius a_i and its position.

As a first approximation one might neglect this correlation, and such an approach has been successfully applied to suspensions of highly charged latex particles,[3,5] where the sizes of the particles have almost no influence on their positions. In this approach one simply substitutes

$$x = 1 - (\overline{a^3})^2/\overline{a^6} \tag{14}$$

or, for not too high polydispersities $\sigma_f \approx 3\sigma_a$, into Eqs. (8)–(10). However, for particles with hard sphere interactions this approach was found[4] entirely inadequate because substitution of Eqs. (14) and (12) into Eq. (10) gave wrong predictions for $S^M(0)$, which has been calculated by Vrij[6] under the Percus–Yevick approximation.

Nevertheless Pusey *et al.*[4] argued that in dynamic light scattering from a polydisperse colloidal system, one still can distinguish two kinds of fluctuations: (i) overall density fluctuations of the colloidal species and (ii) concentration fluctuations at constant overall density. These fluctuation modes can be related to the fluctuating variables that appear in the work of Kirkwood and Goldberg.[7] Adapted to the situation of a colloidal dispersion considered to be in dialytic equilibrium with the solvent (component 0), which is kept at constant chemical potential μ_0, these variables can be written as

$$\lambda_1 = \sum_{k=1}^{r} \overline{V}_k \delta\rho_k \,, \tag{15}$$

$$\lambda_p = \frac{\delta\rho_p}{\rho_p} - \frac{\delta\rho_1}{\rho_1} p = 2,3,\ldots,r \,. \tag{16}$$

Here

$$\overline{V}_k = \left(\frac{\partial V}{\partial N_k}\right)_{T,\Pi,N_{j\neq k}} \,, \tag{17}$$

where V is the volume of the dispersion, Π is the osmotic pressure, N_k is the number of particles of the k th species and ρ_k is the number density of the k th species. It is assumed that the system consists of r colloidal species differing in size, which can be considered as r components.

It can be shown that fluctuations in the osmotic pressure are caused by only λ_1. The fluctuation modes $\lambda_2,\lambda_3,\ldots,\lambda_r$ give rise only to fluctuations in the differences in the chemical potentials of the various species at constant osmotic pressure. Osmotic pressure gradients drive collective diffusion, whereas gradients in chemical potential differences cause exchange diffusion. The process of exchange diffusion, which involves the Brownian displacement of particles over distances larger than their own diameter, is closely related to long-time self-diffusion.

The general polydisperse case is too complex for a detailed calculation of the amplitudes and decay times of the various modes; however, particularly at high concentrations, it may be argued that owing to the different relaxation rates there is little coupling between the collective diffusion mode and the exchange modes. Assuming this to be the case, the amplitude related to collective diffusion is proportional to $\langle \lambda_1^2 \rangle$. The remaining light scattering contribution A_- will relax according to the process of exchange diffusion. More specifically, Eqs. (10) and (11) are generalized to

$$S^M(0) = A_+ + A_- = \frac{\overline{f}^2}{\overline{f^2}} kT\left(\frac{\partial\rho}{\partial\Pi}\right) + A_- \,, \tag{18}$$

where $(\partial\rho/\partial\Pi)$ is the symbol for

$$-\frac{N}{V^2}\left(\frac{\partial V}{\partial\Pi}\right)_{T,\mu_0,N_k} .$$

Expressions for both $S^M(0)$ and $(\partial\rho/\partial\Pi)$ have been obtained for polydisperse systems in the Percus–Yevick approximation.[4] For narrow distributions one finds

$$\frac{S^M(0)}{S^I(0)} = 1 + \frac{3\sigma^2\phi(4-\phi)}{(1-\phi)^2} \tag{19}$$

and

$$\frac{A_+}{S^I(0)} = \left[1 + \frac{3\sigma^2(7\phi^2+8\phi+3)}{(1+2\phi)^2}\right]^{-1} , \tag{20}$$

where $S^I(0)$ is given by Eq. (12). In Fig. 1(b) we plot the relative amplitude $A_-/(A_+ + A_-) = 1 - A_+/S^M(0)$ as a function of volume fraction ϕ for various values of the standard deviation σ_a. These curves should be compared with the curves of Fig. 1(a), i.e., the simple approach with $\sigma_f = 3\sigma_a$.

D. Combined optical and size polydispersity

In general the distribution of scattering powers arises from a distribution in particle size as well as from a distribution in refractive index. The scattering amplitude is $f_i = b_i a_i^3$, where b_i is proportional to the difference between the refractive index of the particle and the dispersing medium $(n_i - n_0)$.

Here we will make the simplifying assumption that there exists no correlation between the distribution in size and the distribution in refractive index. This means that for each species p, comprising all N_p particles with size a_p,

$$\overline{b_p^m} \equiv N_p^{-1} \sum_{\alpha=1}^{N_p} b_\alpha^m = \overline{b^m} \,, \tag{21}$$

and so

$$\overline{f} = \overline{b}\ \overline{a^3} \quad \text{and} \quad \overline{f^2} = \overline{b^2}\ \overline{a^6} .$$

Such a system can be characterized by a standard deviation in size σ_a and a standard deviation in b, σ_b given by

$$\sigma_b^2 = (\overline{b^2} - \overline{b}^2)/\overline{b}^2 .$$

Analogous to Eq. (8) we introduce

$$x = 1 - \overline{b}^2/\overline{b^2} = \sigma_b^2/(1+\sigma_b^2) \tag{22}$$

as a measure of the optical polydispersity.

Inserting $f_i = b_i a_i^3$ into the expression (2) for the measured dynamic structure factor $F^M(q,\tau|\sigma_a,x)$ and following the same resummation procedure that led to Eq. (5) we will find

$$F^M(q,\tau|\sigma_a,x) = (1-x)F^M(q,\tau|\sigma_a,x=0) + xF^s(q,\tau|\sigma_a) \,, \tag{23}$$

where $F^M(q,\tau|\sigma_a,x=0)$ is the measured dynamic structure factor in the absence of optical polydispersity, given by Eq. (13), and

$$F^s(q,\tau|\sigma_a) = [N\,\overline{a^6}]^{-1} \sum_i a_i^6 \langle \exp\{i\mathbf{q}\cdot[\mathbf{r}_i(0) - \mathbf{r}_i(\tau)]\}\rangle \quad (24)$$

is an average self-dynamic structure factor. According to the theory of Pusey *et al.*[4] the term $F^M(q,\tau|\sigma_a,x=0)$ will again be composed of a collective mode and an exchange mode, with their mode amplitudes $A_+(\sigma_a,x=0)$ and $A_-(\sigma_a,x=0)$ given by Eq. (18), which will be rewritten as

$$S^M(0|\sigma_a,x=0) = A_+(\sigma_a,x=0) + A_-(\sigma_a,x=0)\,.$$

In the Percus–Yevick approximation $S^M(0|\sigma_a,x=0)$ and $A_+(\sigma_a,x=0)$ are still given by Eqs. (19), (20), and (12). Thus in the $\tau=0$, $qa\to 0$ limit Eq. (23) reduces to

$$A_{\rm tot} = S^M(0|\sigma_a,x) = [1-x]S^M(0|\sigma_a,x=0) + x = A_+(\sigma_a,x) + A_-(\sigma_a,x)\,, \quad (25)$$

where the amplitude of the collective mode is

$$A_+(\sigma_a,x) = (1-x)A_+(\sigma_a,x=0) \quad (26)$$

and the amplitude of the slow (exchange/self) mode is

$$A_-(\sigma_a,x) = (1-x)A_-(\sigma_a,x=0) + x\,. \quad (27)$$

Explicit expressions for the relative amplitude of the slow mode,

$$\frac{A_-}{A_{\rm tot}} = 1 - \frac{A_+}{A_{\rm tot}} = 1 - \frac{(1-x)A_+(\sigma_a,x=0)}{(1-x)S^M(0|\sigma_a,x=0)+x}\,, \quad (28)$$

are found after substitution of the Eqs. (19), (20), and (12) into (28). In Fig. 1(c) we plot this relative amplitude as a function of volume fraction ϕ for a size polydispersity $\sigma_a = 0.10$ combined with various values of the standard deviation σ_b.

Note that Eq. (25) still retains the general form of Eq. (18), namely

$$S^M(0) = A_{\rm tot} = A_+ + A_-$$

with

$$A_+ = \frac{\bar{f}^2}{\overline{f^2}}\,kT\left(\frac{\partial\rho}{\partial\Pi}\right).$$

In the case that the optical polydispersity and size polydispersity are coupled, one can still use this approach to calculate the mode amplitudes, provided one is able to calculate the measured static structure factor $S^M(0)$.

III. EXPERIMENTAL DETAILS

In order to measure the mode separation we performed DLS measurements on polydisperse systems of small silica particles, sterically stabilized by a coating of stearyl chains, dispersed in cyclohexane at 25 °C. These particles, synthesize according to the method of Van Helden *et al.*,[8] behave like hard sphere model systems.[9]

We compare the data obtained from two dispersions differing only in size and degree of polydispersity of the particles. These systems will hereafter be referred to as systems I and II. The two systems were characterized by DLS measurements on dilute samples. From a second order cumulant expansion[10] an apparent diffusion coefficient (or apparent radius) and polydispersity index were obtained.[4] From these the number-averaged mean radius a_m and standard deviation σ_a were calculated. In this way we found the values $a_m = 11.5 \pm 1.5$ nm and $\sigma_a = 0.30$–0.35 for system I, and for system II we found $a_m = 21$ nm and $\sigma_a = 0.2$. These values of a_m and σ_a are consistent with the results obtained from the apparent radii of gyration as measured by static light scattering. As far as the number-averaged radius is concerned, the above values are also consistent with the values obtained by electron microscopy ($a_m = 9 \pm 1$ nm for system I and $a_m = 23 \pm 3$ nm for system II). On the other hand, we found that the standard deviations as obtained from electron microscopy and small-angle neutron scattering (system II) are significantly lower ($\sigma_a = 0.10$–0.15) than the values obtained from DLS. These differences may possibly be attributed to the presence of clusters of particles in the dispersion. This phenomenon would have a pronounced effect on scattering at low q (light scattering), but rather little influence on scattering at high q (small angle neutron scattering) and electron microscopy. From the residual scattering of dilute samples close to or at the matchpoint, we estimated as an upper limit for the optical polydispersity: $\sigma_b < 0.10$–0.20 (system I) and $\sigma_b < 0.15$–0.20 (system II).

Medium-concentrated stock dispersions were made dust-free by means of filtration through millipore filters of pore diameter 0.22 μm (system I) and 1.2 μm (system II), respectively. The highest particle concentration was obtained by evaporating the solvent from these stock dispersions under dust-free conditions. All light scattering measurements were made with the same cylindrical $\varnothing = 1$ cm cell, and lower particle concentrations were obtained by diluting the sample in this cell with weighed amounts of dust free cyclohexane. As a check the weight fractions were also measured by drying weighed samples taken from the cell. Volume fractions were calculated using the densities of the silica particles and the solvent, 1.58 and 0.774 g cm^{-3}, respectively.

Dynamic light scattering (DLS) measurements were made with an Argon ion laser (Spectra Physics model 165) operating at 514.5 nm. The laser beam was focused in the sample cell, which was placed in a cylindrical refractive index matching bath. The temperature of this surrounding bath was controlled within 0.1 °C. Autocorrelation functions were measured with a Malvern Multibit K7025 128 points correlator. Because the correlator channels are linearly spaced in time, we had to combine a number of successive intensity autocorrelation functions with increasing channel delay time, to cover the whole time span of interest (up to 4 decades). For each concentration, measurements were made at a number of scattering angles to eliminate possible q dependency.

IV. RESULTS AND DISCUSSION

DLS measurements were made up to volume fractions $\phi = 0.55$. In Fig. 2 we present $\ln g^{(1)}(\tau)$ vs τ for various volume fractions ϕ of system I. It turns out that with increasing

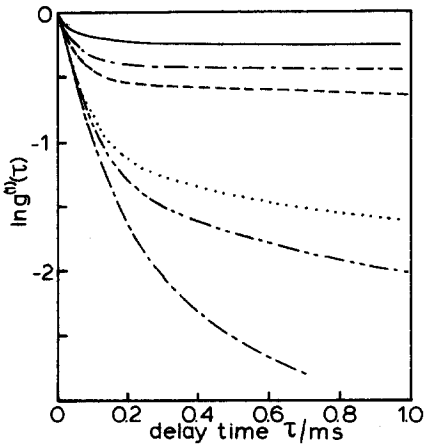

FIG. 2. Logarithm of electric field autocorrelation function vs time for system I for various volume fractions: $\varphi = 0.15$ (- - -); $\varphi = 0.20$ (- - - -); $\varphi = 0.24$ (···); $\varphi = 0.34$ (- - -); $\varphi = 0.40$ (-·-), and $\varphi = 0.46$ (—).

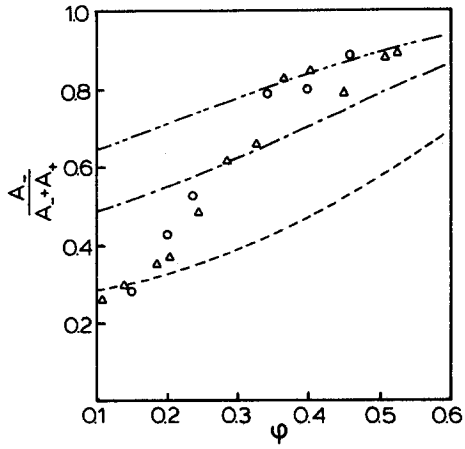

FIG. 3. Relative amplitudes of the slow mode as a function of volume fraction φ for system I (O) and for system II (Δ), compared with theoretical predictions for pure size polydispersity: $\sigma_a = 0.2$ (- - -); $\sigma_a = 0.3$ (- - -), and $\sigma_a = 0.4$ (- - - -).

concentration the measured electric field autocorrelation function definitely consists of a fast- and a slow-decaying part. The amplitudes and initial decays associated with these parts were estimated by fitting a sum of two exponentials to the part of $g^{(1)}(\tau)$ shown in Fig. 2, where the slow mode has hardly decayed. The slow decay is definitely not single exponential and also the fast decay appears to deviate from single-exponential behavior. In order to further characterize the decay of the slow mode we estimated in addition to its initial decay also the overall decay of the slow mode by fitting the tail of $g^{(1)}(\tau)$ to a single exponential. In Table I we present the decay constant of the fast mode and the initial and overall decay constants of the slow mode, all expressed as diffusion coefficients. The decay times associated with the slow and fast parts differ considerably.

The decay time of the slow part increases rapidly with increasing concentration, whereas the fast mode shows little concentration dependence. These results are in qualitative agreement with the available theory, and it seems plausible that the fast and slow modes may be associated with collective and exchange diffusion, respectively.

In Fig. 3 we plot the relative amplitude of the slow (exchange) mode as a function of volume fraction ϕ for both systems studied. The dependence on overall concentration of this amplitude is more pronounced than predicted by the theory of Pusey *et al.*[4] for pure size polydispersity. The trace of the data points shows the characteristics of optical polydispersity. In fact, the shape is better explained by our simple model that takes both optical and size polydispersity into account. In Fig. 4 we compare the relative amplitudes with the predictions of Sec. II D. A reasonable fit can be obtained with a size polydispersity $\sigma_a = 0.10$–0.15 and an optical polydispersity $\sigma_b = 0.25$–0.35. These values for the optical polydispersity are somewhat higher, however, than the values estimated above.

The theoretical analysis assumes a perfect hard-sphere interaction. Part of the differences between experiment and theoretical predictions based on pure size polydispersity (see Fig. 3) could be explained by the effects of the deviations from true hard-sphere interactions. As mentioned in Sec. II C for highly charged particles the mode amplitudes can be calculated satisfactorily[3,5] by treating size polydispersity just as a form of optical polydispersity with $\sigma_f \cong 3\sigma_a$. In that case

TABLE I. Values of the decay constant of the fast mode (D_+) and the range of decay constants of the slow modes (D_-) for system I. Apparent diffusion coefficient at infinite dilution: $D_{app} = 13.4\ 10^{-12}\ m^2/s$.

		$D_-/10^{-12}\ m^2/s$	
ϕ	$D_+/10^{-12}\ m^2/s$	Initial decay	Overall decay
0.15	21.3	3	1
0.20	22.3	0.9	0.45
0.24	23.0	0.6	0.3
0.34	27.7	0.12	0.045
0.40	26.5	0.08	0.016
0.46	31	(<0.08)	0.001

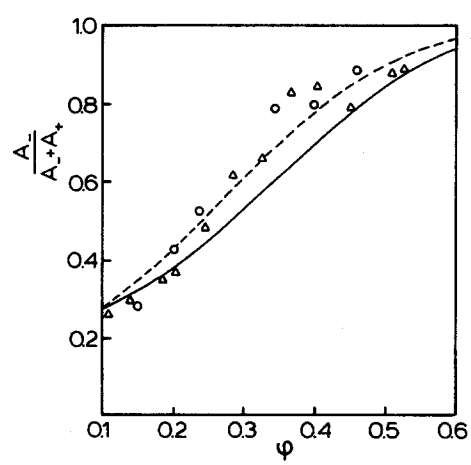

FIG. 4. Relative amplitudes of the slow mode as a function of volume fraction φ for system I (O) and for system II (Δ), compared with theoretical predictions for combined size and optical polydispersity: $\sigma_a = 0.10$ with $\sigma_b = 0.35$ (- - -), and $\sigma_a = 0.15$ with $\sigma_b = 0.25$ (—).

the datapoints should be compared with the curves for $\sigma_f = 0.30$ and $\sigma_f = 0.40$ in Fig. 1(a).

V. CONCLUSIONS

We have studied the influence of polydispersities on the dynamic light scattering by suspensions of particles with hard-sphere interactions at low qa. We have verified the theoretical predictions by performing DLS measurements on dispersions of small, polydisperse particles. For concentrated suspensions of such particles, the measured electric field autocorrelation function is composed of two groups of modes with well separated decay times. The fast mode may be associated with collective diffusion and the slow modes with exchange diffusion.

We have extended the calculation of Pusey *et al.*[4] of the mode amplitudes to the case of combined optical and size polydispersity. The correspondence with the measurements is quite satisfactory in view of the simplicity of the model (no correlation between the optical and size polydispersities) and the uncertainties in the degree and nature of the polydispersities.

The collective diffusion shows little concentration dependence, whereas the exchange diffusion becomes up to 1000 times slower compared to the limit of infinite dilution, indicating that diffusion over distances larger than the diameter of the particles becomes extremely hindered in concentrated dispersions. This observation is reminiscent of the description of the glass transition, where particles become trapped by their local environment. It may explain why dispersions of polydisperse hard spheres at high concentrations so readily form a glass.[11,12]

ACKNOWLEDGMENTS

We thank Mr. S. Coenen for his expert assistance with the DLS measurements and we are grateful to Mr. G. Geels for providing us with the silica spheres of system II. We thank Mrs. M. Uit de Bulten and Mrs. M. de Groot for typing the manuscript. This work is part of the research program of the Foundation for Fundamental Research of Matter (FOM) with financial support from the Netherlands Organisation for Pure Research (ZWO).

[1] P. N. Pusey and R. J. A. Tough, *Dynamic Light Scattering: Applications of Photon Correlation Spectroscopy*, edited by R. Pecora (Plenum, New York, 1985), pp. 85–179.
[2] J. M. Rallison and P. J. Hinch, J. Fluid Mech. **167**, 131 (1986).
[3] M. B. Weissman, J. Chem. Phys. **72**, 231 (1980).
[4] P. N. Pusey, H. M. Fijnaut, and A. Vrij, J. Chem. Phys. **77**, 4270 (1982).
[5] W. Härtl and H. Versmold, J. Chem. Phys. **80**, 1387 (1984).
[6] A. Vrij, J. Chem. Phys. **69**, 1742 (1978).
[7] J. G. Kirkwood and R. J. Goldberg, J. Chem. Phys. **18**, 54 (1950).
[8] A. K. van Helden, J. W. Jansen, and A. Vrij, J. Colloid Interface Sci. **81**, 354 (1981).
[9] A. Vrij, J. W. Jansen, J. K. G. Dhont, C. Pathmamanohavan, M. M. Kops-Werkhoven, and H. M. Fijnaut, Faraday Discuss. Chem. Soc. **76**, 19 (1983).
[10] D. E. Koppel, J. Chem. Phys. **57**, 4814 (1972).
[11] C. G. de Kruif, P. W. Rouw, J. W. Jansen, and A. Vrij, J. Phys. (Paris) **46**, C3-295 (1985).
[12] P. N. Pusey and W. van Megen, Nature (London) **320**, 340 (1986).